

Ozone column classified climatology of ozone and temperature profiles based on ozonesonde and satellite data

L. N. Lamsal, M. Weber, S. Tellmann, and J. P. Burrows

Institute of Environmental Physics, University of Bremen, Bremen, Germany

Received 23 February 2004; revised 17 June 2004; accepted 9 August 2004; published 22 October 2004.

[1] An updated and atmospheric dynamics oriented global climatology of ozone profiles has been derived from ozonesonde and satellite observations. The climatology, which uses total ozone to parameterize the profile shape, provides improved a priori information for ozone profile retrieval from satellite measurements using optimal estimation. It can be also used to correct the profile shape error in total ozone retrieval. Sonde data were selected from the 1990–2000 and 1988–1999 period for SAGE II excluding two years of SAGE II V6.1 data influenced by the Mount Pinatubo eruption in 1991. In addition, POAM III V3 data covering the polar region and SHADOZ ozonesonde data in the tropics were included. The ozone profile data were binned in steps of 30 DU of total ozone, 30° wide zonal bands, and into a six-month season (winter/spring and summer/fall) in middle and high latitudes. No seasonal distinction is needed in the low-latitude region (30°S to 30°N). Mean and standard deviation profiles for each ozone class were combined from satellites and sondes with a transition region in the range 20–26 km to merge both data sets. Temperature data from sonde, SAGE II collocated NMC, and POAM III collocated UKMO, where NMC and UKMO data are used in respective ozone retrieval, have been binned and averaged in the same manner as the ozone profiles so that for each mean ozone profile a matching temperature profile was derived. Corresponding ozone and temperature profiles help in accounting for the temperature dependence of the ozone absorption cross sections in the retrieval process. Key features of both ozone and temperature climatologies are discussed. As examples, ozone-temperature correlation and the climatology of tropopause heights as derived from this climatology are presented, and they serve as diagnostic tools to show that the new climatology is a representative data set for global applications. Good agreement between collocated sonde profiles from Hohenpeissenberg (47.8°, 11.0°) and GOME ozone profiles, retrieved using optimal estimation method and using this climatology as constraints, was found. Also, comparison with GOME results, which were retrieved using a zonal monthly mean climatology, demonstrates the large improvements achieved by using this new climatology, particularly in the lowermost stratosphere and tropopause region. *INDEX TERMS:* 3309 Meteorology and Atmospheric Dynamics: Climatology (1620); *KEYWORDS:* atmospheric dynamics, climatology, ozone

Citation: Lamsal, L. N., M. Weber, S. Tellmann, and J. P. Burrows (2004), Ozone column classified climatology of ozone and temperature profiles based on ozonesonde and satellite data, *J. Geophys. Res.*, 109, D20304, doi:10.1029/2004JD004680.

1. Introduction

[2] A climatology of ozone is of fundamental importance because it provides information on the mean state and variability (covariance) that can be used either as a priori constraint in satellite retrievals or as initial condition for three-dimensional chemical transport models. In addition, it is a source for comparison with models and retrieved data. Traditionally, climatologies of ozone [e.g., Fortuin and Kelder, 1998] and temperature are monthly zonal means and in terms of spatial coordinates. Local [e.g., Yonemura

et al., 2002], regional, and global climatologies exist. *McPeters et al.* [1997] provided a satellite derived monthly zonal mean climatology for the middle and upper stratosphere with the primary purpose of calculating total columns from balloonsonde measurements. A tropospheric ozone climatology was developed by *Logan* [1999a]. This climatology was based on sonde, surface, and satellite data. It provides the two-dimensional (latitude and altitude) ozone field at middle and high latitudes, and three-dimensional (latitude, longitude, and altitude) in the tropics. Aimed for general circulation models, *Fortuin and Kelder* [1998] compiled a two-dimensional climatology of ozone based on ozonesonde and Solar Backscattered Ultraviolet (SBUV) data over a target period of 1980–1991.

[3] Wang *et al.* [1995] showed a large longitudinal asymmetry in ozone values. This results in large differences between zonal mean and local values and might cause a bias when zonal mean is used in an atmospheric model or as a priori state for inversion. Furthermore, a significant level of information can be lost from zonal averaging in this approach. Thus the regional and temporal variability in ozone and temperature makes the preparation of a meaningful climatology a challenge. Wang *et al.* [1995] reported a significant improvement in model results by considering longitudinal variation in ozone.

[4] Austin [1998] suggested a climatology in terms of dynamical based coordinates where the author has shown that the small scale features are present in such climatologies. Using total ozone as dynamical proxy, Klenk *et al.* [1983] derived standard ozone profiles to use them as a priori information for SBUV ozone profile inversion algorithm. For Total Ozone Mapping Spectrometer (TOMS) retrieval, theoretical radiances are computed using standard climatological ozone profiles which were created from SAGE II and balloonsonde data [Wellemeyer *et al.*, 1997].

[5] Prior knowledge on the state space is an essential part of the optimal estimation method [Rodgers, 1976, 2000] which is almost exclusively applied for atmospheric observation. Satellite observation that maps the state space into measurement space is an indirect approach of measurement and an inversion process is required for its solution. A finite number of measurements for obtaining a profile (a continuous function) is an underconstrained nonlinear problem and standard nonlinear least squares methods do not lead to reasonable solutions. The optimal estimation formalism introduced by Rodgers [1976] explicitly uses mean and covariance of the a priori profile together with the measurement error to constrain a poorly constrained solution space consisting of many possible outcomes. The main aim of an a priori constraint is therefore to restrict the components of the solution that are in the null space (unmeasurable part of state space) or near null space (e.g., troposphere) of the weighting function matrix. The hidden information of the null space is required to come from the a priori information, but the components of the state which can be measured well enough are weakly affected by a priori. The structures with short vertical scale of variation are not provided by the inverse method, but the information at such scales comes from the a priori [Coe *et al.*, 2002]. In order to retain all the information, a fine representation and a realistic a priori are needed.

[6] An additional knowledge on the state can also be added as prior information [Rodgers, 2000]. Large variances in the a priori profile as observed in the tropopause region lends no extra information to the inversion. As the monthly mean ozone climatology does not account for interannual variability, there is clearly a need to obtain an improved a priori climatology, which on the one hand represents the large seasonal variability at all altitude levels and, on the other hand, provides variances (and covariances between altitude levels) which are small enough not to destabilise the retrieval. This can be only achieved by creating a climatology providing extra information about the state, where profile classes are sorted by the information like lower stratospheric potential vorticity (PV) or equivalent latitudes. Strong correlations between total ozone and

tropopause height [Appenzeller *et al.*, 2000; Salby and Callaghan, 1993] and total ozone and the height of ozone maximum suggest that total ozone, which contains the information of ozone dynamics and chemistry, can also be used as a dynamical proxy. Preliminary studies [Darmawan, 2002] have shown a significant reduction in ozone class variances by sorting the profiles by total ozone as compared to a monthly zonal mean climatology. Since the use of PV as dynamical proxy can be of problem in the tropics, it is more convenient to use total ozone. This has the following advantages: (1) The retrieval process does not require any meteorological data; (2) total ozone retrieved from the same measurements can be used to select the appropriate a priori climatological profile for ozone profile retrieval.

[7] In addition, features like the dramatic ozone loss in Antarctica [Farman *et al.*, 1985], significant negative trend in midlatitude ozone [Stolarski *et al.*, 1991], and potential sign of ozone recovery [Newchurch *et al.*, 2003] reveal that the ozone climatology should be regularly updated and be based upon recent data sets. The primary goal of the present paper is to provide an updated and atmospheric dynamics oriented ozone and temperature climatologies to be used in ozone retrievals as a priori from Global Ozone Monitoring Experiments (GOME) and SCAning Imaging Absorption spectroMeter for Atmospheric CHartographY (SCIAMACHY) [Burrows *et al.*, 1999; Bovensmann *et al.*, 1999] or any other UV backscatter satellite measurements. First, the total ozone as retrieved by Differential Optical Absorption Spectroscopy (DOAS) technique can be used to select an appropriate climatological profile to be used as a priori information for optimal estimation on ozone profile retrieval [Munro *et al.*, 1998; Hoogen *et al.*, 1999a, 1999b; van der A *et al.*, 2002]. Second, the climatology provides an opportunity to correct the profile shape errors [see Wellemeyer *et al.*, 1997] in total ozone retrievals, especially at high solar zenith angles. The simultaneous use of matching temperature profiles aids in properly accounting for the temperature dependence of the ozone absorption cross sections in the retrieval process.

[8] A wide range of data sources is used in the compilation of this new climatology. Description of the data and method of compilation are discussed in section 2. The frequency distribution of ozone is described in section 3. Composite ozone and temperature climatologies are presented in section 4. The correlation between mean ozone and temperature profiles has been studied and is reported in section 5. A climatology of tropopause heights as a function of total ozone is presented in section 6. Both features show that the new climatology is truly representative of the ozone profile shapes encountered globally in the atmosphere. Comparison between sonde ozone profiles, the results from the climatology, and GOME ozone profiles retrieved using two different ozone profile climatologies as a priori constraints is presented in section 7. A conclusion is given in section 8.

2. Data

2.1. Ozone sonde Data

[9] Data from ozone sonde stations as listed in Tables 1 and 2 were used to prepare this climatology. The majority of the data were obtained from the World Ozone and Ultravi-

Table 1. SHADOZ (Tropical) Stations^a

Station	Latitude	Longitude	Data Period
Paramaribo	5.8°N	55.2°W	1999–2001
San Christobal	0.9°S	89.6°W	1998–2001
Nairobi	1.3°S	36.8°E	1998–2002
Malindi	3.0°S	40.2°E	1999–2002
Natal	5.4°S	35.4°W	1998–2002
Watakosek	7.6°S	112.6°E	1998–2002
Ascension Is.	7.9°S	14.4°W	1998–2002
Am Samoa	14.2°S	170.6°W	1998–2002
Tahiti	18.0°S	149.0°W	1998–1999
Fiji	18.1°S	178.4°E	1998–2002
La Reunion	21.1°S	55.5°E	1998–2002
Irene	25.9°S	28.2°E	1998–2002

^aAll of these stations are using ECC except Watakosek which was using Meisei until the instrument type was changed to ECC.

olet Data Center (WOUDC), Environment Canada, Downsview, Ontario [Fioletov *et al.*, 1999]. The source of data for the tropics was from the Southern Hemisphere Additional Ozonesondes (SHADOZ) [Thompson *et al.*, 2003a, 2003b]. The geographical distribution of those stations is shown in Figure 1. More details about individual stations, seasonal behavior, and trend of ozone can be found in Logan [1985, 1999a, 1999b] and Thompson *et al.* [2003a, 2003b, and references therein].

[10] The majority of stations included in this study have made regular measurements from 1990 to 2000. Five stations, namely, Laverton (from 1989 to 1999), Wallops Island, Sodankylä, Marambio (from 1988 to 1998), and De Bilt (from 1994 to 2001) are from slightly different periods but inclusion of data before 1990 or after 2000 makes them homogeneous in time. Three

stations, Lerwick, Eureka, and Praha, with ozone observations from 1992 to 2001 and Ny Ålesund from 1990 to 1993 were included to increase the geographical coverage. Tropical stations from WOUDC are not considered reliable enough. Their observations are rather irregular and hence were not included. The gap in the tropics was filled by SHADOZ data. Twelve stations were selected, most of them have ozone observations from 1998 to 2002 (see Table 1). The use of only five years of data could be one of the limitations of this climatology, particularly in the tropics.

[11] For the climatology to be representative, an extensive geographical coverage is required. In the northern hemisphere (NH), there are many stations to choose from, and the geographical coverage is quite satisfactory. The situation has been improved significantly in the tropics, particularly in the southern hemisphere (SH), after the establishment of the SHADOZ network. In the northern tropics and in the southern midlatitude and polar regions, only a limited number of stations are available. More stations in these regions are needed for better understanding of ozone distribution, its variation, and long-term trend. Out of 38 stations used in this climatology, northern midlatitude region [30°–60°] alone comprises of 14 stations. Six stations in the northern polar region [60°–90°] and 12 stations in the low latitude [30°S–30°N] have been selected. In the southern hemisphere, only two stations in the midlatitude and three stations in the polar region are available with a sufficient 10-year data record. For the frequency of ozone soundings in each of the stations, the reader is referred to Logan [1999a, 1999b] and Thompson *et al.* [2003a, 2003b].

Table 2. WOUDC Ozonesonde Stations Used in the Compilation of the Climatology

WMO Code	Station	Latitude	Longitude	Type	Data Period
<i>Northern Polar Region</i>					
018	Alert	82.5°N	64.5°W	ECC	1988–1998
315	Eureka	80.0°N	86.2°W	ECC	1992–2001
089	Ny Ålesund	78.9°N	11.9°E	ECC	1990–1993
024	Resolute	74.7°N	94.9°W	ECC	1990–2000
262	Sodankylä	67.3°N	26.5°E	ECC	1988–1998
043	Lerwick	60.1°N	1.2°W	ECC	1992–2001
<i>Northern Midlatitude Region</i>					
021	Edmonton	53.5°N	114.1°W	ECC	1990–2000
076	Goose Bay	53.3°N	60.4°W	ECC	1990–2000
221	Lagionowo	52.4°N	21.0°E	GDR + ECC	1990–2000
174	Lindenberg	52.2°N	14.1°E	GDR + ECC	1990–2000
316	De Bilt	52.1°N	5.2°E	ECC	1994–2001
242	Praha	50.0°N	14.4°E	BM + ECC	1992–2001
099	Hohenpeissenberg	47.8°N	11.0°E	BM	1990–2000
156	Payerne	46.5°N	6.6°E	BM	1990–2000
012	Sapporo	43.1°N	141.3°E	KC	1990–2000
067	Boulder	40.0°N	105.0°W	ECC	1986–1996
107	Wallops Island	37.9°N	75.5°W	ECC	1988–1998
014	Tateno	36.1°N	140.1°E	KC	1990–2000
007	Kagoshima	31.6°N	130.6°E	KC	1990–2000
<i>Southern Midlatitude Region</i>					
254	Laverton	37.8°S	144.7°E	ECC	1989–1999
256	Lauder	45.0°S	169.7°E	ECC	1990–2000
<i>Southern Polar Region</i>					
233	Marambio	64.2°S	56.7°W	ECC	1988–1998
101	Syowa	69.0°S	39.6°E	KC	1990–2000
323	Neumayer	70.6°S	8.2°W	ECC	1992–2002

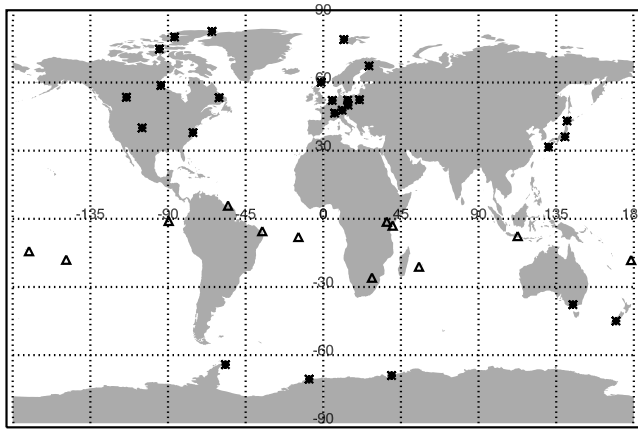


Figure 1. Geographical distribution of the ozonesonde stations. Stars and triangles show the location of WUOUC and SHADOZ sonde stations, respectively.

[12] Most of the stations used Electrochemical Concentration Cell (ECC) [Komhyr, 1969] which has been well validated [Smit *et al.*, 1997; De Backer *et al.*, 1998]. Two European stations, Hohenpeissenberg and Payerne use Brewer Mast (BM) [Brewer and Milford, 1960]. Lindenberg and Legionowo changed the instrument type from the German Democratic Republic (GDR) sonde [Ronnebeck and Milford, 1976] to ECC sonde in June 1992 and 1993, respectively. The GDR sondes produce larger O_3 mixing ratio than either BM or ECC sondes [Logan, 1999a]. Four Japanese stations use their own sonde (KC) which is similar to the Carbon Iodide (CI) sonde of Komhyr [1969]. All these instruments have different precision, accuracy, and different sources of error. A number of comparison campaigns were held to compare the performance of these instruments [Attmanspracher and Dütsch, 1970, 1981; Chanin, 1983; Hilsenrath *et al.*, 1986; De Backer *et al.*, 1995, 1998], but the different campaigns came out with different results. The comparison based on duosounding [De Backer *et al.*, 1998] shows that BM sensors read 10–15% higher in the troposphere, almost the same value at the height of ozone maximum, and 5% less at about 10hPa than ECC sensors. Such differences led to a general practice of correcting the ozonesonde profiles by introducing correction factors (CF). This procedure introduces errors [Logan, 1985; Tiao *et al.*, 1986; McPeters *et al.*, 1997] in the so-called corrected sonde values, and the issue of using correction factors is still ongoing [World Meteorological Organization (WMO), 1998]. In the current climatology it has not been applied. The temperature and pressure data were obtained from radiosondes flown together with ozonesondes. The radiosonde temperatures form a reliable data set which have a reproducibility of about 0.2 K [Knudsen *et al.*, 1996].

[13] Sonde profiles are classified based on the understanding of spatial and temporal variability of ozone. Total ozone exhibits a strong annual cycle. The cycle possesses a characteristic late-winter/early-spring maximum and broad late-summer/early-fall minimum [Eder and LeDuc, 1999; Weber *et al.*, 2003]. The driving force for the annual cycle in ozone is likely to be dynamical in nature: mass transport of

ozone from tropical (source) region to higher latitudes [Bojkov *et al.*, 1994; Holton *et al.*, 1995] and seasonal variance of tropopause height [Stanford *et al.*, 1995]. Photochemistry is another factor for total ozone variation which is solar zenith angle dependent. The profile data have been classified with respect to three effective dimensions: latitude, e.g., low latitude (30°S – 30°N), midlatitude (30° – 60°), and polar (60° – 90°), season (winter/spring and summer/fall) and total ozone. Northern winter/spring and summer/fall are defined as being December–May and June–November periods, respectively. A seasonal distinction was not made for low latitude profiles. The individual ozonesonde reading in units of partial pressure at various pressure levels were converted into number density units and volume mixing ratio at various heights. The values at the end points, i.e., at 0 km and 27 km were determined by assuming a constant mixing ratio from their nearest values. The 0 to 27 km range was then divided into 18 layers each 1.5 km wide. The mean for each layer was calculated and the missing values in the intermediate layers, if any, were determined by spline interpolation. The same treatment was undertaken for the temperature profiles. The column amount of ozone was calculated by integrating the ozone amount up to 27 km and extending it up to 60 km by using a zonal monthly mean ozone climatology (TOMS V8 climatology, (G. Labow, NASA GSFC, personal communication, 2001)) that is based on recent ozonesonde and SAGE II data (1990–2000). The ozonesonde profiles were classified by the hybrid (ozonesonde plus climatological extension) ozone column amount in intervals of 30 DU. The mean and standard deviation profiles for ozone (number density and mixing ratio) and temperature were determined for each (ozone amount) class. Note that the climatological profile above 27 km can differ from the true state of ozone and this difference can introduce some error in the hybrid ozone column amount.

2.2. Satellite Data

[14] Stratospheric Aerosol and Gas Experiment II (SAGE II) and Polar Ozone and Aerosol Measurement III (POAM III) ozone profile data were used to construct the stratospheric ozone profiles. SAGE II aboard the Earth Radiation Budget Satellite (ERBS) has been providing high resolution ozone profile data since October 1984 with a short interruption of about three months in July 2002 [Wang *et al.*, 2002]. SAGE II provides 15 sunrise and 15 sunset measurements each day. The SAGE II spatial coverage extends over a latitude range of approximately 70°S to 70°N having month to month variability. The number of the winter/fall profiles in the northern hemisphere and spring/summer profiles in the southern hemisphere beyond 60° latitude are limited. POAM data is a good available extension to prepare stratospheric climatological profiles in the polar region. POAM III instrument [Lucke *et al.*, 1999] on the Pour l’Observation de la Terre (SPOT) 4 satellite makes 14 to 15 measurements per day in each hemisphere. Because of the satellite inclination of 98.7° , the POAM III measurement latitudes vary from 55°N to 73°N in the northern hemisphere and from 63°S to 88°S in the southern hemisphere.

[15] Ten years of SAGE II V6.1 data from 1988 to 1999 were included in the new climatology. SAGE II V6.1 data were not available after middle of 2000 due to an altitude registration problem. The SAGE II ozone retrieval requires

the separation of ozone absorption and aerosol extinction [Steele and Turco, 1997]. Thus, in spite of improvements in the V6.1 retrieval [Wang *et al.*, 2002] algorithm, ozone retrievals from SAGE II data are biased in the lower stratosphere when aerosol extinction is large, e.g., after the eruption of Mount Pinatubo in mid-July 1991. For this reason the 1991 and 1992 data are not included in the new climatology.

[16] The source of temperature data in the SAGE II operational data is the routine gridded data analyses from the National Meteorological Center (NMC). The temperature data which are based on radiosonde and National Oceanic and Atmospheric Administration (NOAA) operational satellites were used to extend the sonde temperature climatology up to the upper stratosphere. The temperature data as used for the POAM III retrieval were obtained from the UK Meteorological Office (UKMO) which were interpolated to the time and location of the POAM III measurements.

[17] An analysis performed by Wang *et al.* [2002] to assess the SAGE II V6.1 data quality shows that SAGE II and coincident ozonesonde agree in the mean to better than 10% down to the tropopause. SAGE II provides useful data up to 60 km [Cunnold *et al.*, 1989; Attmanspracher *et al.*, 1989] with an expected accuracy of 6% above 25 km altitude. The difference between the sunrise and sunset ozone values are interpreted to be approximately 5%. Validation studies [Lumpe *et al.*, 2002; Danilin *et al.*, 2002; Randall *et al.*, 2003] using ECC sonde data, and aircraft (ER-2) and space-based measurement (SAGE II, HALOE) show that POAM III V3 ozone values agree to within 5 to 7% in the altitude range from 13 to 60 km and a larger disagreement (10 to 15%) is observed below 13 km. The quality of NMC [Wang *et al.*, 1992] and UKMO [Pullen and Jones, 1997] temperature data is believed to be poorer at higher altitudes because of the use of satellite data in their data assimilation system.

[18] SAGE II data (for tropics and midlatitude region) were taken from 60 km down to 14 km and POAM III data (for polar region) from 60 to 8 km removing profiles with missing values within the range. The use of satellite data almost down to tropopause is of great significance for the accuracy of climatology because it takes into account the most dynamically sensitive region where short-term ozone variations are controlled to a large extent by horizontal and vertical transport [Salby and Callaghan, 1993]. SAGE II V6.1 and POAM III V3 ozone profile data sets were extended below 14 km and 8 km, respectively, by means of the TOMS V8 climatology to evaluate the ozone column amount by integration. The ozone number density, which both data set provide, were converted to volume mixing ratio in order to construct the stratospheric ozone mixing ratio climatology. As in the case of the sonde data, satellite profiles were classified by region (tropics, midlatitude, and polar), season (winter/spring and summer/fall), and total ozone (30 DU bins). Mean and standard deviation profiles for ozone and temperature for each of the ozone classes and seasons were calculated.

3. Ozone Frequency Distribution

[19] The frequency distribution of total ozone corresponding to the profiles collected in the data set has

been determined and evaluated. The distribution function of total ozone depends on various atmospheric perturbations such as changes in dynamics, stratospheric chemistry, solar activity, etc. It yields the information about the most probable value and the distribution of extreme values [Reck *et al.*, 1996]. The frequency distribution, as shown in Figure 2, shows the percentage frequency for a given ozone class of 30 DU width for the satellite and sonde data separately. The frequency distributions of all GOME V3.0 total ozone data from middle of 1995 through 2002 are also shown in Figure 2, and it approximates the global distribution due to the larger sampling size of GOME as compared to SAGE II, POAM III, and sondes. Effect of different sampling size, interannual variation, and the effect of the instrumental/retrieval differences are expected to affect ozone distribution, but Figure 2 shows that sonde and satellite data distributions closely approximate that given by GOME total ozone. Integrated ozone values have about the same range of values as given by GOME. The agreement in total ozone distribution obtained from two entirely independent sources confirms the good representation of the global ozone field in the new climatology and justifies the methodology with which the climatology was prepared.

[20] The frequency distribution is wider in winter/spring and narrower in summer/fall. Temperature gradients and the resulting short-term total ozone variation are stronger in winter than in summer owing to the variation of the solar insolation and variation in planetary activity driving ozone transport into high latitudes [Fusco and Salby, 1999; Randel *et al.*, 2002; Weber *et al.*, 2003]. In tropics the distribution is narrow and symmetric around 250–280 DU. Except in SH polar region where maximum frequency lies in the 280–310 DU range in both winter/spring and summer/fall seasons, the winter/spring distribution has a peak that is shifted to higher total ozone with respect to the summer/fall distribution. Ozone values in late spring and early winter are reflected in the tails of either side of summer/fall ozone distribution. This is because the separation into different half years (Dec.–May, Jun.–Nov.) is somewhat arbitrary and some of the profile shapes are common to both. Larger differences in profile shape are expected in low total ozone classes (ozone hole condition vs. summer/fall profiles).

[21] In SH polar region the asymmetry on the low ozone side is due to chemical depletion of ozone (“ozone hole”) in the Antarctic vortex during polar spring. Very low total ozone cases are also observed in the SH midlatitude region. Earlier studies [e.g., Pérez *et al.*, 2000; Callis *et al.*, 1997] also reported the events of low total ozone. Medium-scale baroclinic disturbances distort the Antarctic vortex and can lead to excursion into midlatitudes. Advection of ozone-poor polar air into the midlatitudes after the final vortex break up has been observed and can also contribute [Randel and Wu, 1995]. Particularly in SH midlatitude, the use of satellite data compensates for the lack of suitable stations covering these low ozone cases.

4. Composite Ozone and Temperature Profile Climatologies

4.1. Ozone

[22] The current climatology is compiled by merging the corresponding mean sonde and satellite profiles. Before

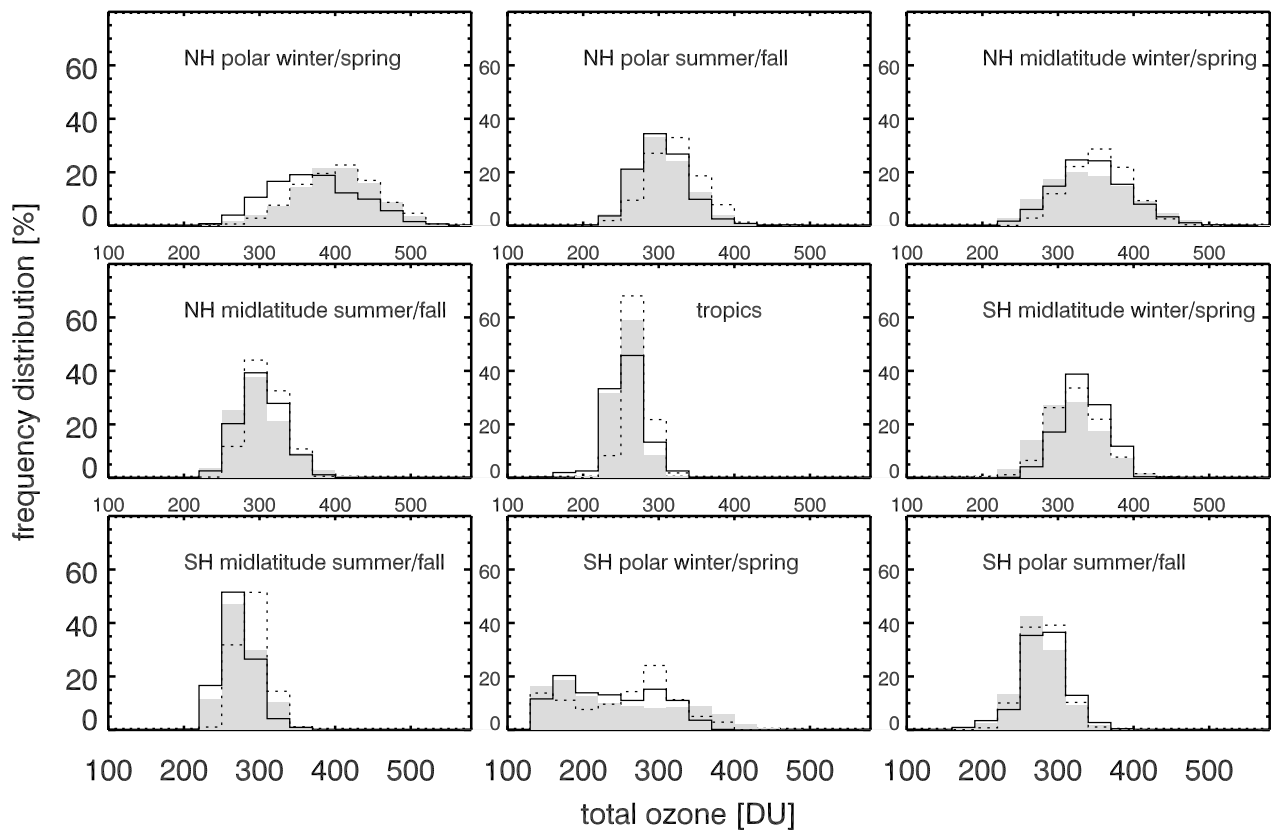


Figure 2. Frequency distribution of total ozone as obtained by integrating sonde (solid line) and satellite (dotted line) profiles and GOME V3.0 data for GOME period 1995–2002 (shaded region).

combining both data sets, sonde values were interpolated into the same altitude grid (1 km) as that of the satellite data. The interpolation was performed for both ozone number density and volume mixing ratio profiles. Mean sonde and satellite ozone profiles for 340–369 DU class of NH midlatitude winter/spring are shown in Figure 3 as an example. A smooth transition between 20 and 26 km was introduced by applying a sliding average. As can be seen in Figure 3, the sonde and satellite climatologies agree well. Some difficulties were encountered at the minimum ozone class for satellite data of SH midlatitude region during winter/spring season where no sonde counterpart was available. Those profiles were extended from 14 km down to 0 km by using the corresponding mean sonde profile from the polar region. The final profiles were scaled, where necessary, to the class mean total ozone values. An identical compilation technique was followed for the climatology of standard deviation.

[23] Figure 4 shows the results of the new dynamics oriented ozone climatology. NH midlatitude and polar regions both have 11 profiles in winter/spring and 7 profiles in summer/fall seasons. This difference is the result of strong planetary activity which cause the total ozone amount vary more strongly in winter/spring. The total ozone amounts are higher in the northern than in the southern hemisphere, which appears to be consistent with the greater transport of ozone in NH [Holton *et al.*, 1995]. SH polar winter/spring comprises of 8 profiles which includes the typical ozone hole profiles as well. Including ozone depleted profiles, which were particularly obtained from satellite

data, SH midlatitude winter/spring comprises of 10 ozone profiles. In summer/fall, there are 5 profiles in midlatitude and 6 in polar region. In the tropics, five profile classes are identified.

[24] The main features of the ozone distributions are clearly seen in this figure. These features include: decrease in the height of ozone maximum with increase in latitude

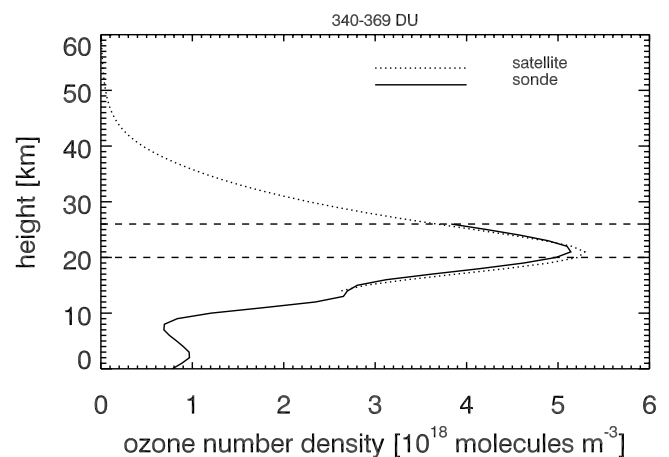


Figure 3. Merging of sonde and satellite profiles. This is the mean profile of 340–369 DU ozone class for NH midlatitude region during winter/spring. Two horizontal lines at 20 and 26 km show the transition region where the sliding averaging is applied.

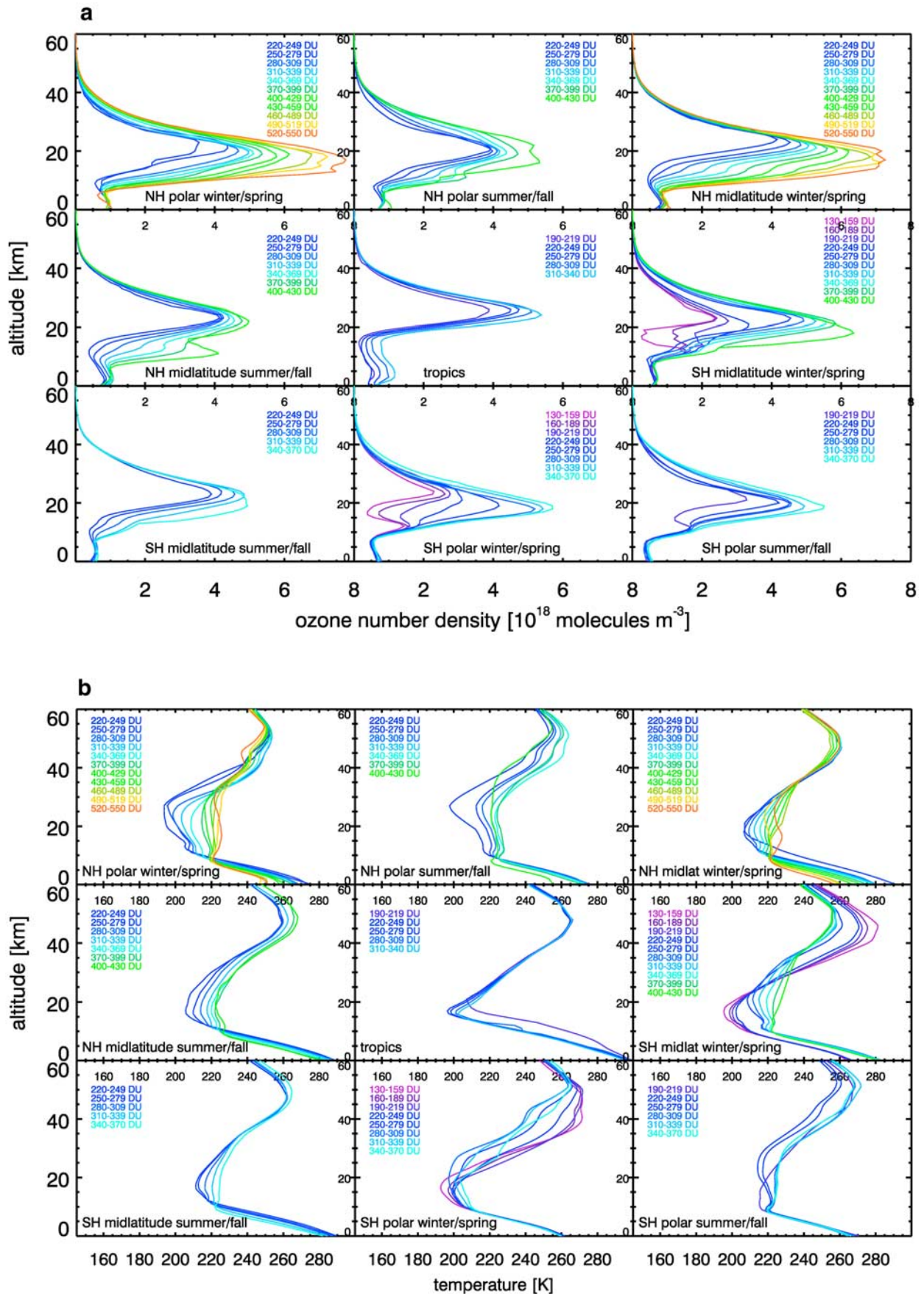


Figure 4. (a) Total ozone classified mean ozone and (b) corresponding temperature profiles.

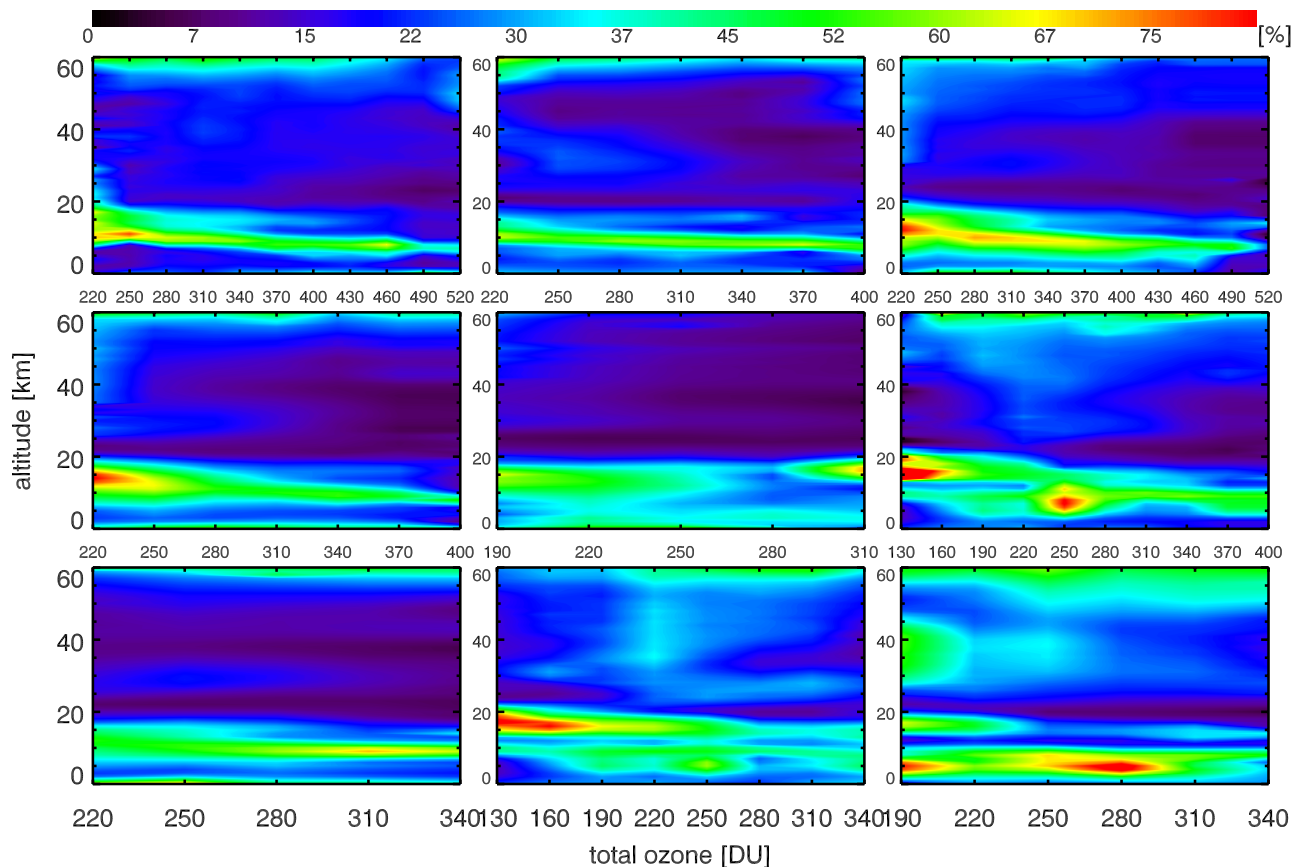


Figure 5. Variability of ozone (in %) as a function of altitude and total ozone. Variability is highest in the lowermost stratosphere and upper troposphere. The plots are located in the same order as in Figures 2 and 4a–4b (i.e., first row left to right: NH polar winter/spring, NH polar summer/fall, NH midlatitude winter/spring; second row: NH midlatitude summer/fall, tropics, SH midlatitude winter/spring; third row: SH midlatitude summer/fall, SH polar winter/spring, SH polar summer/fall).

and total ozone, sharp ozone gradients between the vertically stratified lower stratosphere and well mixed troposphere, and Antarctic ozone hole profile in spring in SH polar and ozone depleted profile in SH midlatitude region. Many midlatitude profiles exhibit filamentation or a secondary maximum. This figure clearly shows the hemispheric and seasonal differences in tropospheric ozone which causes profiles of the same ozone class in both hemispheres to differ in the stratosphere. For example, the tropospheric ozone level in the southern hemisphere is, in general, less than in the northern hemisphere. For the same total ozone value, southern hemispheric stratospheric ozone level should be higher than in the NH. In the SH, tropospheric ozone levels do not vary as much as in the northern hemisphere. This could be the result of stronger anthropogenic emission in NH, weaker meridional circulation, or underrepresentation of ozonesonde stations in SH. Figure 4 also shows that the tropospheric column in tropics are highly variable in line with total column variation. This result is in agreement with SHADOZ tropospheric ozone climatology [Thompson *et al.*, 2003a, 2003b] that was based on three years of data.

[25] Figure 5 shows the variability defined as (standard deviation)/mean \times 100% of ozone. The variability lies below 30% except in the lowermost stratosphere and upper troposphere where the variability is typically up to 60%.

This value can increase to 80% during austral spring in southern hemisphere. The large variance in this region is the result of combined contribution from dynamical activity, tropospheric-stratospheric exchange, and the chemical depletion of ozone. The increase in variability in altitude above 40 km may to some extent come from satellite sunrise/sunset differences (sunrise values being higher) and errors in the satellite retrieval algorithm [Wang *et al.*, 1992]. The variability patterns, in general, differ for solstice conditions: low values occurring in summer hemisphere and high in winter hemisphere.

[26] Large ozone variability is observed in the midlatitude region for low ozone cases (220–280 DU, for example). It is likely due to the fact that the high tropopause profile (subtropical origin) and ozone depleted profile (polar origin) can have same total ozone amount but different profile shapes. Similar cases are observed in the polar region where early-summer/late-fall profiles and ozone hole profiles belong to the same ozone class.

4.2. Temperature

[27] The climatology derived from radiosonde data was combined with the climatology based on meteorological analyses (NMC and UKMO) data set by merging the corresponding ozone class mean temperature profiles using the same sliding average scheme as applied for ozone. The

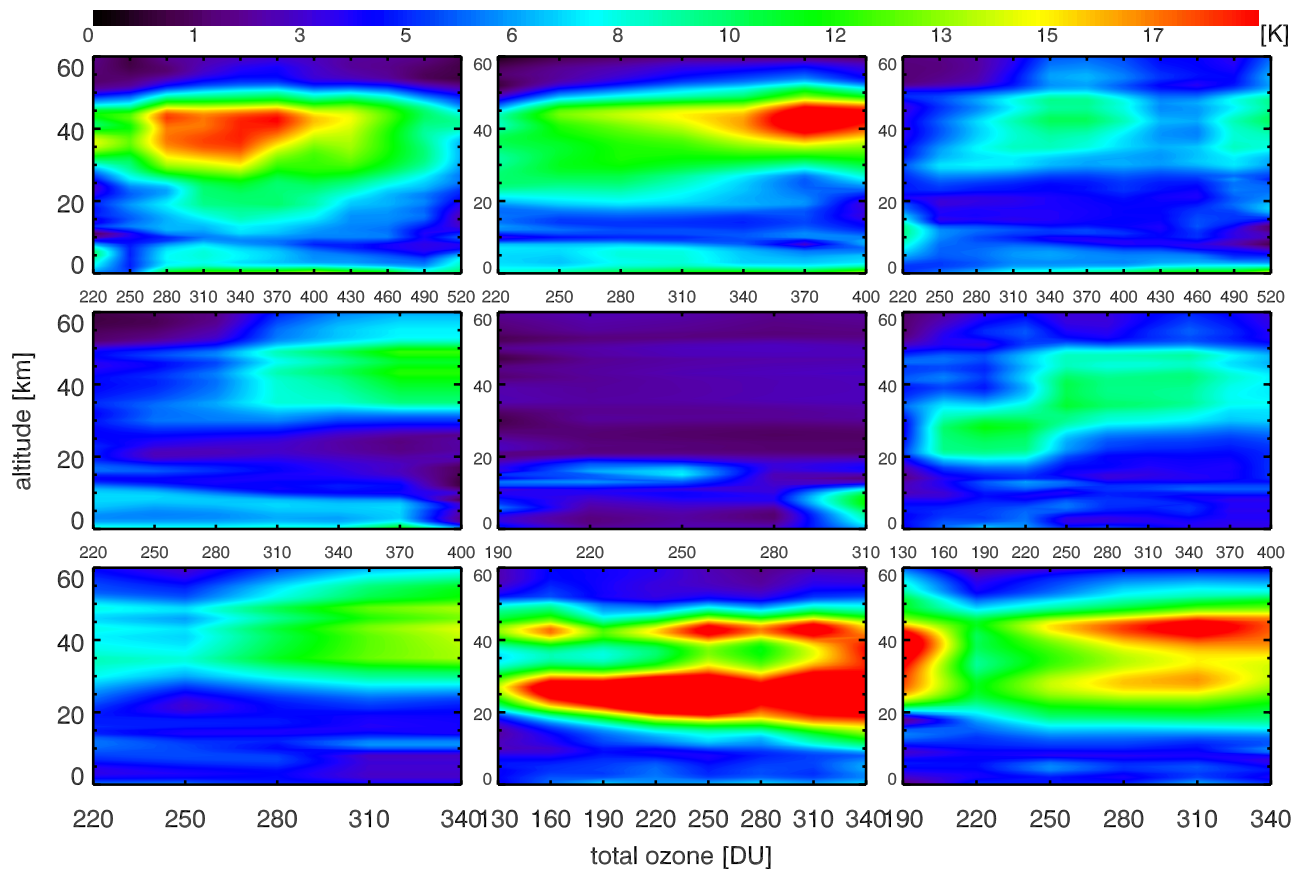


Figure 6. Temperature standard deviation (in K) as a function of altitude and total ozone. The plots are located in the same order as in Figure 5.

sonde values were spline interpolated to the 1 km altitude grid. For cases when matching sonde profile were missing, the met analyses were extended down to the surface.

[28] Mean temperature profiles are shown in Figure 4. One of the important features seen in the figure is that the profiles with low tropopause are associated with a cold troposphere, warm lower stratosphere, and high total ozone amount. An identical feature, known as stratosphere-troposphere compensation, has been identified by *Steinbrecht et al.* [1998] when the author classified temperature and ozone profiles by tropopause height. In NH midlatitude winter/spring, for example, the temperature for 220–249 DU in troposphere (at surface) is higher than that for 400–429 DU by about 19 K while in the lower stratosphere (19 km) the temperature for 400–429 DU is higher by about 14 K. As seen in this figure, the magnitude of difference differs with seasons, being largest in winter/spring. Furthermore, the difference in temperature between ozone classes decrease with increasing stratospheric altitude and decreasing tropospheric altitude. In the upper stratosphere, no clear pattern of variation could be identified; the reasons for this behavior are not understood, and further investigation is required.

[29] As explained by *Fels* [1982], the Arctic lower stratosphere is warmer than that in the Antarctic. In SH polar region, especially during winter/spring, the lower stratospheric mean temperature falls as low as 193 K leading to severe ozone depletion as shown in Figure 4. The figure shows that the low-ozone events in the SH

midlatitude region is accompanied by the decrease in the mean temperature of the lower stratosphere as low as 195.5 K. It is likely due to the fact that the fixed latitude of 30°S to 60°S is arbitrary which occasionally samples the vortex air in the midlatitude. The horizontal advection of cold air from Antarctic latitudes could also result in such low-temperature events [*Pérez et al.*, 2000]. Another interesting feature that can be seen in the present climatology is the sharp tropical tropopause temperature minimum which has been pointed out by *Randel et al.* [2003].

[30] The standard deviation for the composite temperature climatology is shown in Figure 6. The profiles were obtained from the standard deviation profiles of sonde and met analyses data by the same method as applied to the mean temperature profiles. The standard deviation lies below 14 K in the midlatitude region and becomes as high as 25 K in the polar region during winter/spring. The variance in the upper stratosphere could be explained by the out of phase variation relationship between ozone and temperature [*Smith*, 1995]. In the lower stratosphere, the temperature variation is dominantly controlled by transport [e.g., *Rood and Douglass*, 1985]. The large variability in the polar region could be due to the use of relatively smaller sample size of five years. Note that UKMO data have been used in the polar region and the quality of UKMO temperature decreases with increasing altitude possibly due to the poorer quality of radiosonde temperature and increased use of satellite data. QBO (Quasi-biennial Oscillation), solar

cycle, tropopause height variation, etc. also contribute to temperature variability.

5. Ozone and Temperature Correlation

[31] Figure 7, as an example, shows the correlation coefficient profile based on the mean ozone and temperature profiles for NH midlatitude winter/spring. The ozone is negatively correlated with temperature above 35 km, positively correlated between 35 and 10 km, and negatively correlated below 10 km. This result is in good agreement with the model calculated correlation [Rood and Douglass, 1985] between ozone and temperature.

[32] The main aim of investigating this type of correlation is to show that the new ozone and temperature climatologies presented here is capable of reproducing the known relationships between ozone and temperature. If these relationships do not hold, it would indicate that either the methodology has faults or the climatology is not a true representation of the global ozone distribution.

[33] The interpretation of the observed correlation is not easy in the kind of studies presented here because the correlation profile shown in Figure 7 is based on mean profiles and no other attempts are made to separate the factors which can contribute in the ozone-temperature correlation. Nevertheless, in the upper stratosphere ozone concentration is photochemically controlled. The destruction of odd oxygen ($O_3 + O$) by various chemical reactions (Chapman chemistry and catalytic cycles) can vary strongly with temperature. An increase in temperature will increase the rate at which ozone is destroyed, so ozone and temperature are negatively correlated. The detail of the explanation on the physical mechanism on ozone temperature relationship in the upper stratosphere can be found in Smith [1995]. In the lower stratosphere, transport dominates over photochemistry [Brosseur and Solomon, 1984]. There are two main mechanisms whereby the lower stratospheric ozone and temperature are positively correlated. First, radiative effect: high ozone concentration helps to maintain a persistent temperature through the absorption of solar and terrestrial radiative energy [Miller et al., 1992]. Second, dynamical effect: transport of air parcel and adiabatic compression at high latitudes lead to increase in ozone and temperature [Wirth, 1993; Petzoldt et al., 1994; Fortuin and Kelder, 1996].

6. Climatology of Tropopause Height

[34] The mean state of tropopause height for each of the ozone classes has been analysed. This provides the mean relationship between total ozone and tropopause height. Investigation of the link between total ozone and tropopause height itself is a broad field but the basic idea of the present study is to verify if the new climatology of ozone and temperature reproduces the existing knowledge on tropopause height in a climatological sense.

[35] Tropopause marks the location of an abrupt transition in the temperature lapse rate [WMO, 1957], in the values of potential vorticity (PV) [e.g., Zängl and Wirth, 2000], and in the concentration of chemical species like ozone [Bethan et al., 1998]. Various tropopause definitions have been identified. Hoinka [1998], however, has shown that the tropo-

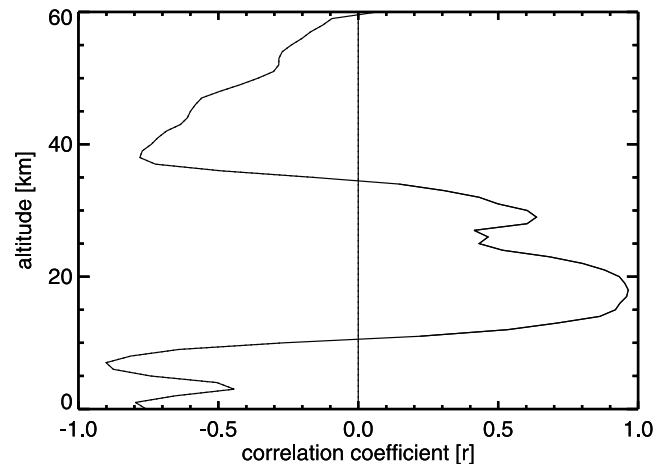


Figure 7. Correlation between mean ozone and temperature for NH midlatitude winter/spring as function of altitude.

pause height as evaluated from different definitions provide similar results. In the present study, the tropopause height as provided by NMC data were used for the low and midlatitude regions. It is calculated using the same algorithm as used by National Centers for Environmental Prediction (NCEP) (J. M. Zawodny, personal communication, 2003) for the location of SAGE II measurement. Similar to ozone and temperature profiles, corresponding tropopause heights were classified by total ozone amount and the mean tropopause heights were calculated for both winter/spring and summer/fall seasons. In the polar region where data come from a different source the position of thermal tropopause was estimated by using the WMO [1957] definition. Thermal tropopause is the lowest level at which the temperature lapse rate decreases to 2 K per km or less, provided the average lapse rate between this level and all higher levels within 2 km does not exceed 2 K per km. In all cases the location of ozone tropopause was evaluated by applying the criterion developed by Bethan et al. [1996]. The threshold value of ozone gradient where ozone tropopause lies is 60 ppb/km at conditions that the ozone mixing ratio exceed 80 ppb and that the values immediately above the tropopause exceed 110 ppb.

[36] Table 3 shows how the tropopause (TTP, thermal tropopause; OTP, ozone tropopause) height changes with ozone column amount. Figure 8, as an example, shows how tropopause height and tropospheric ozone vary with total ozone. As apparent in the climatology, various authors [Hoinka et al., 1996; Steinbrecht et al., 1998; Birner et al., 2002] have reported the correlation between the tropopause height and the stratospheric ozone column. Increase in the height of tropopause cause the stratospheric column to decrease. The strength of correlation, however, depends upon the region and season [Krzyścin et al., 1998]. In summer/fall, the increase of total ozone for 1 km decrease in tropopause height is larger than in winter/spring. Besides its relation with stratospheric column, the tropopause height is also sensitive to surface temperature [Forster and Shine, 1997]. Santer et al. [2003] suggested that the increase in the tropopause height is associated with stratospheric cooling due to stratospheric ozone loss.

Table 3. Climatology of Tropopause Height^a

Total Ozone, DU	Type	NHP-WS	SHP-WS	NHP-SF	SHP-SF	NHM-WS	SHM-WS	NHM-SF	SHM-SF	LL
145	TTP	-	12.0	-	-	-	12.8	-	-	-
	OTH	-	10.1	-	-	-	10.0	-	-	-
175	TTP	-	11.4	-	-	-	12.2	-	-	-
	OTH	-	9.6	-	-	-	9.6	-	-	-
205	TTP	-	11.3	-	11.6	-	11.6	-	-	17.3
	OTH	-	9.8	-	8.6	-	9.7	-	-	17.0
235	TTP	12.4	10.9	10.9	11.5	14.4	11.5	13.7	13.3	16.5
	OTH	11.5	9.5	12.5	9.1	15.0	9.5	14.9	14.9	16.7
265	TTP	11.6	11.0	10.3	11.5	13.3	12.2	13.0	12.9	16.3
	OTH	11.2	9.6	10.0	8.8	13.9	11.1	14.0	14.5	16.5
295	TTP	11.0	10.5	11.0	11.5	12.0	11.7	12.3	11.2	15.7
	OTH	9.9	9.5	9.4	8.2	11.2	10.9	13.4	13.7	16.3
325	TTP	10.6	10.0	9.4	11.5	11.1	11.1	11.3	9.7	14.5
	OTH	9.3	9.3	8.6	8.2	10.3	10.3	10.6	12.1	15.2
355	TTP	9.7	9.7	9.0	11.4	10.3	10.2	10.7	9.0	-
	OTH	8.6	8.9	8.1	8.1	9.5	9.5	9.2	10.7	-
385	TTP	9.1	-	8.6	-	9.5	9.5	9.6	-	-
	OTH	8.1	-	7.8	-	8.8	9.0	8.2	-	-
415	TTP	8.7	-	7.6	-	9.0	9.1	8.6	-	-
	OTH	7.8	-	7.1	-	8.1	9.0	7.4	-	-
445	TTP	8.3	-	-	-	8.6	-	-	-	-
	OTH	7.5	-	-	-	7.8	-	-	-	-
475	TTP	8.2	-	-	-	8.4	-	-	-	-
	OTH	7.5	-	-	-	7.4	-	-	-	-
505	TTP	7.9	-	-	-	7.8	-	-	-	-
	OTH	7.1	-	-	-	7.3	-	-	-	-
535	TTP	7.6	-	-	-	7.7	-	-	-	-
	OTH	6.7	-	-	-	6.9	-	-	-	-

^aTropopause types: TTP, thermal tropopause; OTH, ozone tropopause. Regional bins: NHP, northern polar; SHP, southern polar; NHM, northern midlatitude; SHM, southern midlatitude; LL, low latitude. Seasonal bins: WS, winter/spring; SF, summer/fall.

[37] The tropopause height shows a considerable north south variability but without any clear symmetry between northern and southern hemisphere. The most probable reason for such asymmetry is related to the difference in the distribution of land and ocean in the two hemispheres. A sharp and cold tropopause is observed in the tropics which was also observed by *Highwood and Hoskins* [1998]. As expected, the tropopause height is usually higher in summer/fall than in winter/spring in midlatitude region [e.g., *Hoinka et al.*, 1996]. However, in polar region the corresponding summer/fall ozone tropopause (OTH) is lower than that of winter/spring. This fact is also reported by *Hoinka* [1998]. If the thermal tropopause is considered, the same behavior is observed in the NH, but not in the SH.

[38] *Bethan et al.* [1996] evaluated the difference between thermal and ozone tropopause. Based on stations located between 51°N and 79°N, they showed that the ozone tropopause lies about 0.5 km below the thermal tropopause. With few exceptions (e.g., SH polar summer/fall, and extreme ozone cases) this feature is reflected in the climatology.

7. Ozone Profile Retrieval: A Case Study

[39] The Full Retrieval Method (FURM) [*Hoogen et al.*, 1999a, 1999b] developed for the nadir viewing GOME [*Burrows et al.*, 1999] has been used to assess the performance of the new climatology. This ozone profile retrieval algorithm is based on the optimal estimation scheme that includes a priori profiles in order to stabilize the iterative ozone retrieval [*Rodgers*, 2000]. In the optimal estimation approach, the atmospheric state vector is adjusted in iterative

steps in order to minimize the weighted sum of squares between measured and modeled Sun-normalized radiances and between the modeled and the a priori parameters. In the $(i + 1)$ th iteration, the estimate x_{i+1} is given by

$$x_{i+1} = x_a + \left(K_i^T S_y^{-1} K_i + S_a^{-1} \right)^{-1} \times K_i^T S_y^{-1} [y - y_i + K_i(x_i - x_a)], \quad (1)$$

where x_i and x_{i+1} are the calculated atmospheric state vectors, here the ozone profile, after i th and $(i + 1)$ th

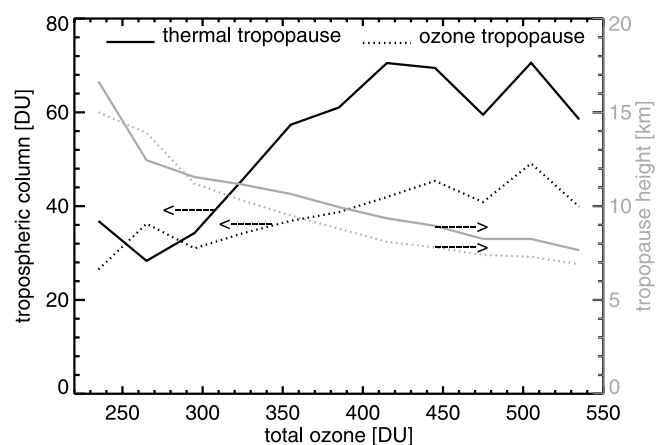


Figure 8. Climatology of tropopause height for NH midlatitude winter/spring. It shows the mean relationship between total ozone, tropopause height, and tropospheric column.

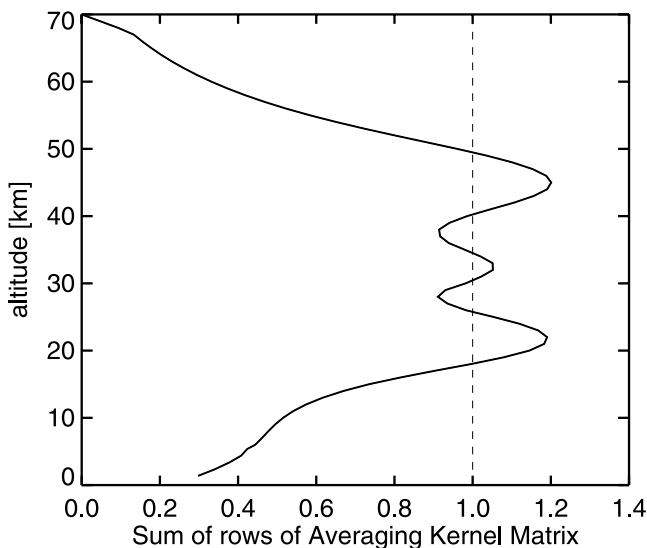


Figure 9. Sum of rows of averaging kernel matrix as an indicator for the sensitivity to the measurement. Values larger than about 1 indicate significant contribution from the measurements, while lower values indicate stronger weighting toward the a priori value.

iterations, respectively, which yield the retrieval solution \hat{x} after the convergence is achieved. The logarithm of Sun-normalized radiance as measured by GOME is y . y_i is the same quantity calculated with the radiative transfer model GOMETRAN [Rozanov *et al.*, 1997], x_a is the a priori atmospheric state, S_a and S_y are the measurement error covariance and the a priori covariance matrix, respectively, and K_i is the weighting function matrix after i th iteration.

[40] The sum of rows of the averaging kernel matrix,

$$A_i = \left(K_i^T S_y^{-1} K_i + S_a^{-1} \right)^{-1} K_i^T S_y^{-1} K_i, \quad (2)$$

is an indicator for the sensitivity of the retrieval to the measurement as shown in Figure 9. The information content is low below 15 km and above 50 km and in these altitude ranges climatological ozone information is of critical importance.

[41] Figure 10 shows a comparison between GOME vertical ozone profiles derived with the zonal monthly mean ozone climatology from *Fortuin and Kelder* [1998], on the one hand, and the new climatology presented in this paper, on the other, with results from collocated ozone sondes launched in Hohenpeissenberg (47.8°, 11.0°, 50 profiles) during 1997. The mean profile of the new climatology agrees to better than 10% with the mean sonde profile with a root mean square of the mean relative deviation being less than 20% in most cases except in the tropopause. The difference between mean of the zonal monthly mean climatology and averaged sonde results from Hohenpeissenberg in the tropopause region is up to 40% and a factor of four higher compared to result from

our climatology. The retrieved mean GOME profile shows a significant improvement in the troposphere by using our updated climatology presented here. Despite the improvement of the GOME retrieval using the new climatology a positive bias in the GOME-sonde mean differences in the lowermost stratosphere remain. This can be explained by the asymmetric averaging kernels that smooth the GOME profiles. In the lowermost stratosphere contribution from the ozone maximum increases the retrieved ozone down to

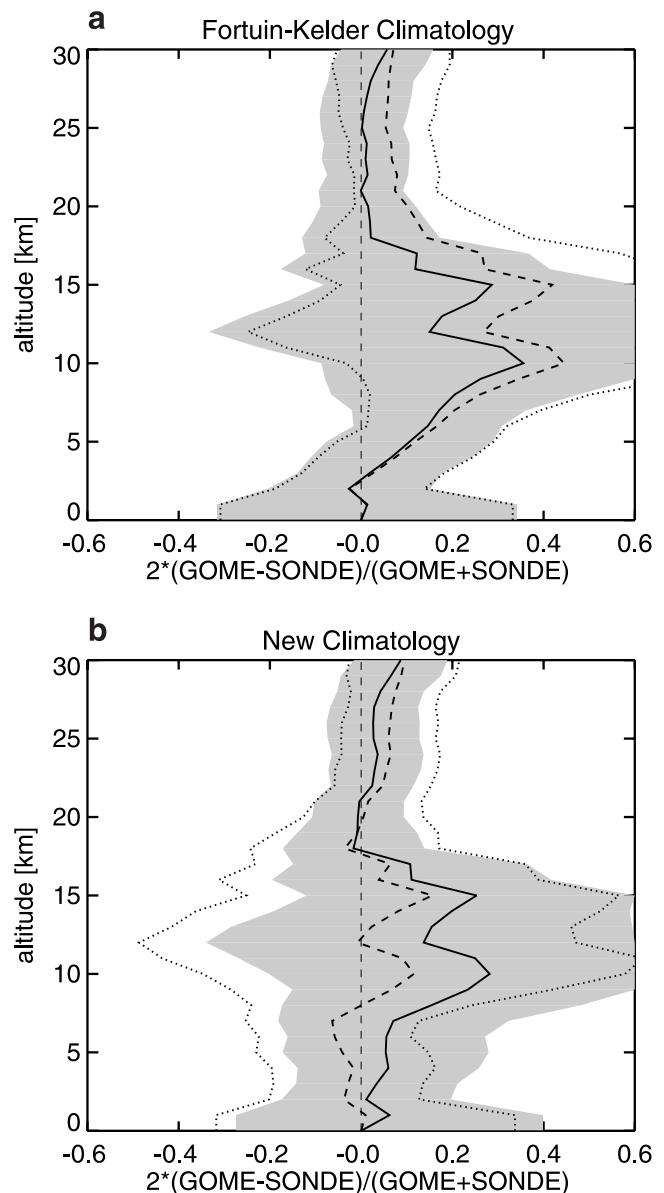


Figure 10. Mean relative deviation between retrieved GOME and ozone sonde profiles (solid line) and between climatological and ozone sondes profiles (dashed line), respectively, for the year 1997 in Hohenpeissenberg (50 profiles). The profiles were retrieved using (a) zonal monthly mean climatology and (b) our climatology. The shaded region shows the root mean square of mean relative deviation for the retrieval, and the dotted line shows that of our climatology.

the tropopause region [Hoogen *et al.*, 1999a; Meijer *et al.*, 2003].

8. Concluding Remarks

[42] Ozone column classified ozone and temperature climatologies at six month long seasonal and 30° wide latitude bins have been derived using large volume of recent ground-based and satellite data. The resulting set of ozone profiles is presented in Figure 4, and their variances are shown in Figures 5 and 6.

[43] The climatologies were developed with the aim of improving the quality of a priori information. They are intended to be used for the ozone column and profile retrieval from GOME, SCIAMACHY, and their future generation like GOME-2. Separation of ozone profiles by column amount, what is used as a proxy for an atmospheric dynamics, has been proven to reduce the variances in the tropopause region compared to the traditional zonal monthly mean climatology. This helps to stabilize the fit results in the profile retrieval. A case study pursued at Hohenpeissenberg has demonstrated a good use of our climatology. Profile shape and matching temperature profile as additional information may also improve the accuracy of the retrieved ozone column [Wellemeyer *et al.*, 1997].

[44] The strong point of this climatology is the separation into hemispheres and semiannual cycles. The semiannual cycle allows a better distinction of profiles associated with low total ozone that is dominated by chemically depleted ozone in winter/spring while in summer/fall it is related to the photochemical decay resulting in different profile shapes for the same total ozone class. The use of POAM III data in the polar region and SHADOZ sonde data in the tropics has significantly improved the global representation of the ozone field. Nevertheless, the climatology needs to be regularly updated as the maturity of data sets in polar (satellite data), SH midlatitude regions and northern tropics (both ground-based) increases in order to account for the long-term changes in the ozone field. This climatology can be downloaded from <http://www.iup.physik.uni-bremen.de/gome/o3climatology>.

[45] **Acknowledgments.** We are very grateful to G. Labow, NASA GSFC, for providing TOMS V8 zonal monthly mean ozone profile climatology. We thank WOUDC, SHADOZ, SAGE II, and POAM III teams for providing the data. Finally, we would like to thank the two reviewers for their valuable comments. This work has been supported in part by the GOMSTRAT project within the German Atmospheric Research Program 2000 (AFO 2000) and the University of Bremen.

References

- Appenzeller, C., A. K. Weiss, and J. Staehelin (2000), North Atlantic Oscillation modulates total ozone winter trends, *Geophys. Res. Lett.*, *27*, 1131–1134.
- Attmanspracher, W., and H. U. Dütsch (1970), International ozonesonde intercomparison at the observatory Hohenpeissenberg, January 19 to February 5, 1970, *Ber. Dtsch. Wetterdienstes*, *16*.
- Attmanspracher, W., and H. U. Dütsch (1981), Second international ozonesonde intercomparison at the observatory Hohenpeissenberg, April 5–20 1978, *Ber. Dtsch. Wetterdienstes*, *18*.
- Attmanspracher, W., J. De La Noe, D. De Muer, J. Lenoble, G. Megie, J. Pelon, P. Pruvost, and R. Reiter (1989), European validation of SAGE II ozone profiles, *J. Geophys. Res.*, *94*, 8461–8466.
- Austin, J. (1998), Some ideas on the further development of a stratospheric ozone climatology, *Adv. Space Res.*, *21*, 1393–1402.
- Bethan, S., G. Vaughan, and S. J. Reid (1996), A comparison of ozone and thermal tropopause heights and the impact of tropopause definition on quantifying the ozone content of the troposphere, *Q. J. R. Meteorol. Soc.*, *122*, 929–944.
- Bethan, S., G. Vaughan, C. Gerbig, A. V. Thomas, H. Richer, and D. A. Tiddeman (1998), Chemical air mass differences near fronts, *J. Geophys. Res.*, *103*, 13,413–13,434.
- Birner, T., A. Dörnbrack, and U. Schumann (2002), How sharp is the tropopause at midlatitude?, *Geophys. Res. Lett.*, *29*(14), 1700, doi:10.1029/2002GL015142.
- Bojkov, R. D., V. E. Fioletov, and A. M. Shalamjansky (1994), Total ozone changes over Eurasia since 1973 based on reevaluated filter ozonometer data, *J. Geophys. Res.*, *99*, 22,985–22,999.
- Bovensmann, H., J. P. Burrows, M. Buchwitz, J. Frerick, S. Noël, V. V. Rozanov, K. V. Chance, and A. H. P. Goede (1999), SCIAMACHY - Mission objectives and measurement modes, *J. Atmos. Sci.*, *56*(2), 127–150.
- Brasseur, G., and S. Solomon (1984), *Aeronomy of the Middle Atmosphere*, 441 pp., D. Reidel, Norwell, Mass.
- Brewer, A. W., and J. R. Milford (1960), The Oxford-kew ozonesonde, *Proc. R. Soc. London, Ser. A*, *256*, 470–495.
- Burrows, J. P., et al. (1999), The Global Ozone Monitoring Experiment (GOME): Mission concept and first scientific results, *J. Atmos. Sci.*, *56*, 151–175.
- Callis, L. B., M. Natarajan, J. D. Lambeth, and R. E. Boughner (1997), On the origin of midlatitude ozone changes: Data analysis and simulations for 1979–1993, *J. Geophys. Res.*, *102*, 1215–1228.
- Chanin, M. L. (1983), The intercomparison ozone campaign held in France in June 1981 - Description of the campaign, *Planet Space. Sci.*, *31*, 707–713.
- Coe, H., B. J. Allan, and J. M. C. Plane (2002), Retrieval of vertical profiles of NO₃ from zenith sky measurements using an optimal estimation method, *J. Geophys. Res.*, *107*(D21), 4587, doi:10.1029/2002JD002111.
- Cunnold, D. M., W. P. Chu, R. A. Barnes, M. P. McCormick, and R. E. Veiga (1989), Validation of SAGE II ozone measurements, *J. Geophys. Res.*, *94*, 8447–8460.
- Danilin, M. Y., et al. (2002), Comparison of ER-2 aircraft and POAM III, MLS, and SAGE II satellite measurements during SOLVE using traditional correlative analysis and trajectory hunting technique, *J. Geophys. Res.*, *107*, 8315, doi:10.1029/2001JD000781. [printed 108(D5), 2003]
- Darmawan, A. (2002), Improved dynamical climatology of ozone for use in optimal estimation retrieval, Master thesis, Univ. of Bremen, Bremen, Germany.
- De Backer, H., E. Schoubs, and M. Allaart (1995), Comparison of Brewer Mast and ECC ozonesonde profiles at Uccle and De Bilt, in *Proceedings of the Third European Workshop on Polar Stratospheric Ozone*, edited by J. A. Pyle, N. R. P. Harris, and G. T. Amanatidis, pp. 512–515, Eur. Comm., Brussels.
- De Backer, H., D. De Muer, and G. De Saelaer (1998), Comparison of ozone profiles obtained with Brewer-Mast and Z-ECC sensors during simultaneous ascents, *J. Geophys. Res.*, *103*, 19,641–19,648.
- Eder, B. K., and S. K. LeDuc (1999), A climatology of total ozone mapping spectrometer data using rotated principal component analysis, *J. Geophys. Res.*, *104*, 3691–3709.
- Farman, J. C., B. G. Gardiner, and J. D. Shanklin (1985), Large losses of total ozone in Antarctica reveal seasonal ClO_x/NO_x interaction, *Nature*, *315*, 207–210.
- Fels, S. B. (1982), A parameterization of scale-dependent radiative damping rates in the middle atmosphere, *J. Atmos. Sci.*, *39*, 1141–1152.
- Fioletov, V. E., J. B. Kerr, E. W. Hare, G. J. Labow, and R. D. McPeters (1999), An assessment of the world ground-based total ozone network performance from the comparison with satellite data, *J. Geophys. Res.*, *104*, 1737–1748.
- Forster, P. M. de F., and K. P. Shine (1997), Radiative forcing and temperature trends from stratospheric ozone trends, *J. Geophys. Res.*, *102*, 10,841–10,855.
- Fortuin, J. P., and H. Kelder (1996), Possible links between ozone and temperature profiles, *Geophys. Res. Lett.*, *23*, 1517–1520.
- Fortuin, J. P., and H. Kelder (1998), An ozone climatology based on ozonesondes and satellite measurements, *J. Geophys. Res.*, *103*, 31,709–31,734.
- Fusco, A. C., and M. L. Salby (1999), Interannual variation of total ozone and their relationship to variations of planetary wave activity, *J. Clim.*, *12*, 1619–1629.
- Highwood, E. J., and B. J. Hoskins (1998), The tropical tropopause, *Q. J. R. Meteorol. Soc.*, *124*, 1579–1604.
- Hilsenrath, E., et al. (1986), Results from the Balloon Ozone Intercomparison Campaign (BOIC), *J. Geophys. Res.*, *91*, 13,137–13,152.
- Hoinka, K. P. (1998), Statistics of the global tropopause pressure, *Mon. Weather Rev.*, *126*, 3303–3325.
- Hoinka, K. P., H. Claude, and U. Köhler (1996), On the correlation between tropospheric pressure and ozone above central Europe, *Geophys. Res. Lett.*, *23*, 1753–1756.

- Holton, J. R., P. H. Haynes, M. E. McIntyre, A. R. Douglass, R. B. Rood, and L. Pfister (1995), Stratosphere-troposphere exchange, *Rev. Geophys.*, *33*, 403–439.
- Hoogen, R., V. V. Rozanov, and J. P. Burrows (1999a), Ozone profiles from GOME satellite data: Algorithm description and first validation, *J. Geophys. Res.*, *104*, 8263–8280.
- Hoogen, R., V. V. Rozanov, and J. P. Burrows (1999b), O₃ profiles from GOME satellite data-I: Comparison with ozonesonde measurements, *Phys. Chem. Earth.*, *24*, 447–452.
- Klenk, K. F., P. K. Bhartia, E. Hilsenrath, and A. J. Fleig (1983), Standard ozone profiles from balloon and satellite data sets, *J. Clim. Appl. Meteorol.*, *22*, 2012–2022.
- Knudsen, B. M., J. M. Rosen, N. T. Kjøme, and A. T. Whitten (1996), Comparison of analyzed stratospheric temperatures and calculated trajectories with long-duration balloon data, *J. Geophys. Res.*, *101*, 19,137–19,146.
- Komhyr, W. D. (1969), Electrochemical concentration cells for gas analysis, *Ann. Geophys.*, *25*(1), 203–210.
- Krzyścin, J. W., M. Degórska, and B. R. Więch (1998), Seasonal acceleration of the rate of the total ozone decreases over central Europe: Impact of tropopause height changes, *J. Atmos. Sol. Terr. Phys.*, *60*, 1755–1762.
- Logan, J. A. (1985), Tropospheric ozone: Seasonal behavior, trends, and anthropogenic influence, *J. Geophys. Res.*, *90*, 10,463–10,482.
- Logan, J. A. (1999a), An analysis of ozonesonde data for the troposphere: Recommendations for testing 3-D models and development of a gridded climatology for tropospheric ozone, *J. Geophys. Res.*, *104*, 16,115–16,150.
- Logan, J. A. (1999b), An analysis of ozonesonde data for the lower stratosphere, *J. Geophys. Res.*, *104*, 16,151–16,170.
- Lucke, R. L., et al. (1999), Polar Ozone and Aerosol Measurement (POAM) III instrument and early validation results, *J. Geophys. Res.*, *104*, 18,785–18,799.
- Lumpe, J. D., et al. (2002), Comparison of POAM III ozone measurements with correlative aircraft and balloon data during SOLVE, *J. Geophys. Res.*, *107*, 8316, doi:10.1029/2001JD000472. [printed 108(D5), 2003]
- McPeters, R. D., G. J. Labow, and B. J. Johnson (1997), A satellite-derived ozone climatology for balloonsonde estimation of total column ozone, *J. Geophys. Res.*, *102*, 8875–8885.
- Meijer, Y. J., R. J. van der A, R. F. van Oss, D. P. J. Swart, and H. M. Kelder (2003), Global Ozone Monitoring Experiment ozone profile characterization using interpretation tools and lidar measurements for intercomparison, *J. Geophys. Res.*, *108*(D23), 4723, doi:10.1029/2003JD003498.
- Miller, A. J., R. M. Nagatani, G. C. Tiao, X. F. Niu, G. C. Reinsel, D. J. Wuebbles, and K. Grant (1992), Comparison of observed ozone and temperature trends in the lower stratosphere, *Geophys. Res. Lett.*, *19*, 929–932.
- Munro, R., R. Siddans, W. J. Reburn, and B. J. Kerridge (1998), Direct measurement of tropospheric ozone distributions from space, *Nature*, *392*, 168–171.
- Newchurch, M. J., E.-S. Yang, D. M. Cunnold, G. C. Reinsel, J. M. Zawodny, and J. M. Russell (2003), Evidence for slowdown in stratospheric ozone loss: First stage of ozone recovery, *J. Geophys. Res.*, *108*(D16), 4507, doi:10.1029/2003JD003471.
- Pérez, A., E. Crino, I. Aguirre de Cárcer, and F. Jaque (2000), Low-ozone events and three-dimensional transport at midlatitudes of South America during springs of 1996 and 1997, *J. Geophys. Res.*, *105*, 4553–4561.
- Petzoldt, K., B. Naujokat, and K. Neugeboren (1994), Correlation between stratospheric temperature, total ozone, and tropospheric weather systems, *Geophys. Res. Lett.*, *21*, 1203–1206.
- Pullen, S., and R. L. Jones (1997), Accuracy of temperatures from UKMO analysis of 1994/1995 in the arctic winter stratosphere, *Geophys. Res. Lett.*, *24*, 845–848.
- Randall, C. E., et al. (2003), Validation of POAM III ozone: Comparisons with ozonesonde and satellite data, *J. Geophys. Res.*, *108*(D12), 4367, doi:10.1029/2002JD002944.
- Randel, W. J., and F. Wu (1995), TOMS total ozone trends in potential vorticity coordinates, *Geophys. Res. Lett.*, *22*, 683–686.
- Randel, W. J., F. Wu, and R. Stolarsky (2002), Changes in column ozone correlated with EP flux, *J. Meteorol. Soc. Jpn.*, *80*, 849–862.
- Randel, W. J., F. Wu, and R. R. Waleska (2003), Thermal variability of the tropical tropopause region derived from GPS/MET observations, *J. Geophys. Res.*, *108*(D1), 4024, doi:10.1029/2002JD002595.
- Reck, R. A., B. L. Weinberg, R. M. Bornick, G. Wen, and J. E. Frederick (1996), A new approach to the characterization of long-term changes in total atmospheric ozone: Determination and application of frequency distributions, *Atmos. Environ.*, *30*, 2627–2636.
- Rodgers, C. D. (1976), Retrieval of atmospheric temperature and composition from remote measurements of thermal radiation, *Rev. Geophys.*, *14*, 609–624.
- Rodgers, C. D. (2000), *Inverse Methods for Atmospheric Sounding: Theory and Practice*, Ser. Atmos. Ocean. Planet. Phys., vol. 2, World Sci., River Edge, N. J.
- Ronnebeck, R., and J. R. Milford (1976), Eine weiterentwickelte electrochemische Ozonradiosonde, *Z. Meteorol.*, *26*, 15–19.
- Rood, R. B., and A. R. Douglass (1985), Interpretation of ozone temperature correlations: 1. Theory, *J. Geophys. Res.*, *90*, 5733–5743.
- Rozanov, V. V., D. Diebel, R. J. D. Spurr, and J. P. Burrows (1997), GOMETRAN: A radiative transfer model for the satellite project GOME—The plane parallel version, *J. Geophys. Res.*, *102*, 16,683–16,695.
- Salby, M. L., and P. F. Callaghan (1993), Fluctuations of total ozone and their relationship to stratospheric air motions, *J. Geophys. Res.*, *98*, 2715–2728.
- Santer, B. D., et al. (2003), Behavior of tropopause height and atmospheric temperature in models, reanalyses, and observations, *J. Geophys. Res.*, *108*(D1), 4002, doi:10.1029/2002JD002258.
- Smit, H. G. J., et al. (1997), JOSIE: The 1969 WMO international intercomparison of ozonesondes under quasi flight conditions in the environmental simulation chamber, in *Proceedings of the 18th Quadrennial Ozone Symposium*, edited by R. Bojkov and G. Visconti, Parco Sci. and Technol., D'Abruzzo, Italy.
- Smith, A. K. (1995), Numerical simulation of global variations of temperature, ozone, and trace species in the stratosphere, *J. Geophys. Res.*, *100*, 1253–1269.
- Stanford, J. L., J. R. Ziemke, R. D. McPeters, A. J. Krueger, and P. K. Bhartia (1995), Spectral analyses, climatology, and interannual variability of Nimbus 7 TOMS version 6 total column ozone, *NASA Ref. Publ.*, 1360.
- Steele, H. M., and R. P. Turco (1997), Separation of aerosol and gas components in the Halogen Occultation Experiment and the Stratospheric Aerosol and Gas Experiment (SAGE) II, extinction measurements: Implications for SAGE II ozone concentrations and trends, *J. Geophys. Res.*, *102*, 19,665–19,682.
- Steinbrecht, W., H. Claude, U. Köhler, and K. P. Hoinka (1998), Correlation between tropopause height and total ozone: Implications for long-term changes, *J. Geophys. Res.*, *103*, 19,183–19,192.
- Stolarski, R. S., R. D. McPeters, J. R. Herman, and P. Bloomfield (1991), Total ozone trends deduced from Nimbus 7 TOMS data, *Geophys. Res. Lett.*, *18*, 1015–1018.
- Thompson, A. M., et al. (2003a), Southern Hemisphere Additional Ozonesondes (SHADOZ) 1998–2000 tropical ozone climatology: 1. Comparison with Total Ozone Mapping Spectrometer (TOMS) and ground-based measurements, *J. Geophys. Res.*, *108*(D2), 8238, doi:10.1029/2001JD000967.
- Thompson, A. M., et al. (2003b), Southern Hemisphere Additional Ozonesondes (SHADOZ) 1998–2000 tropical ozone climatology: 2. Tropospheric variability and the zonal wave-one, *J. Geophys. Res.*, *108*(D2), 8241, doi:10.1029/2002JD002241.
- Tiao, G. C., G. C. Reinsel, J. H. Pedrick, G. M. Allenby, C. L. Mateer, A. J. Miller, and J. J. DeLuisi (1986), A statistical trend analysis of ozonesonde data, *J. Geophys. Res.*, *91*, 13,121–13,136.
- van der A, R. J., R. F. van Oss, A. J. M. Pijters, J. P. F. Fortuin, Y. J. Meijer, and H. M. Kelder (2002), Ozone profile retrieval from recalibrated Global Ozone Monitoring Experiment data, *J. Geophys. Res.*, *107*(D15), 4239, doi:10.1029/2001JD000696.
- Wang, H. J., D. M. Cunnold, L. W. Thomason, J. M. Zawodny, and G. E. Bodeker (2002), Assessment of SAGE version 6.1 ozone data quality, *J. Geophys. Res.*, *107*(D23), 4691, doi:10.1029/2002JD002418.
- Wang, P. H., M. P. McCormick, W. P. Chu, J. Lenoble, R. M. Nagatani, M. L. Chanin, R. A. Barnes, F. Schmidlin, and M. Rowland (1992), SAGE II stratospheric density and temperature retrieval experiment, *J. Geophys. Res.*, *97*, 843–863.
- Wang, W.-C., X.-Z. Liang, M. P. Duden, D. Pollard, and S. L. Thompson (1995), Atmospheric ozone as a climate gas, *Atmos. Res.*, *37*, 247–256.
- Weber, M., S. Dhomse, F. Wittrock, A. Richter, B.-M. Sinnhuber, and J. P. Burrows (2003), Dynamical control of NH and SH winter/spring total ozone from GOME observations in 1995–2002, *Geophys. Res. Lett.*, *30*(11), 1583, doi:10.1029/2002GL016799.
- Wellemeyer, C. G., S. L. Taylor, C. J. Seftor, R. D. McPeters, and P. K. Bhartia (1997), A correlation for the total ozone mapping spectrometer profile shape errors at high latitude, *J. Geophys. Res.*, *102*, 9029–9038.
- Wirth, V. (1993), Quasi-stationary planetary waves in total ozone and their correlation with lower stratospheric temperature, *J. Geophys. Res.*, *98*, 8873–8882.

- World Meteorological Organization (WMO) (1957), Definition of the tropopause, *WMO Bull.*, 6, 136.
- World Meteorological Organization (WMO) (1998), Assessment of trends in the vertical distribution of ozone, *WMO Rep. 43*, Global Ozone Res. and Monit. Proj., Geneva.
- Yonemura, S., H. Tsuruta, S. Kawashima, S. Sudo, L. C. Peng, L. S. Fook, Z. Johar, and M. Hayashi (2002), Tropospheric ozone climatology over Peninsular Malaysia from 1992 to 1999, *J. Geophys. Res.*, 107(D15), 4229, doi:10.1029/2001JD000993.
- Zängl, G., and V. Wirth (2000), Synoptic-scale variability of the polar and subpolar tropopause: Data analysis and idealized PV inversions, *Q. J. R. Meteorol. Soc.*, 126, 1–999.
-
- J. P. Burrows, L. N. Lamsal, S. Tellmann, and M. Weber, Institute of Environmental Physics, University of Bremen FB1, P.O. Box 330 440, D-28334 Bremen, Germany. (lamsal@iup.physik.uni-bremen.de)